JOURNAL OF VIROLOGY, Aug. 1970, p. 243-252
Vol. 6, No. 2

Morphogenesis of the Nucleoprotein of Vesicular Stomatitis Virus

BARBARA A. ZAJAC AND KLAUS HUMMELER

Division of Experimental Pathology, The Children's Hospital of Philadelphia, Department of Pediatrics, Medical School, University of Pennsylvania, Philadelphia, Pennsylvania 19146

Received for publication 12 June 1970

Accumulation of the nucleoprotein of vesicular stomatitis virus (VSV) in the cytoplasm of BHK-21 cells and in two of four human cell lines was demonstrated. Appearance and progression of the nucleoprotein inclusions paralleled development of virus-specific immunofluorescence and production of virus progeny. The inclusions appeared early as discrete foci of filamentous material which eventually increased in size to form large masses which replaced normal cytoplasmic constituents. The filamentous strands were found in close proximity to budding virions. The inclusion material was extracted from infected cells and purified in cesium chloride gradients. The isolated filaments resembled the ribonucleoprotein isolated from purified virions. They incorporated ^{3}H-uridine, exhibited virus-specific complement-fixing activity, had a buoyant density of 1.32 g/cm^3, and appeared as single wavy strands the width of which varied from 2.5 to 8.5 nm, depending on the angle of viewing.

The morphology of vesicular stomatitis virus (VSV) has been investigated extensively (6, 8, 10, 14, 17). The ribonucleoprotein of the virus, which is contained in the virion in helical form, has also been analyzed for its morphological, physical, and chemical properties (2, 13, 15, 19, 21). Little is known, however, about the morphogenesis of the ribonucleoprotein of this virus.

Studies concerned with the morphogenesis of the ribonucleoprotein of rabies, a virus morphologically similar to VSV, have shown that accumulation of the ribonucleoprotein as cytoplasmic inclusions is a regular occurrence. It has also been found that the size of these inclusions depended on the strain of rabies virus employed and the type of host cell used for infection (11). The finding of "rabies-like" inclusions in VSV-infected calf kidney cells (17) suggested that the morphogenesis of the ribonucleoprotein of VSV also might be readily investigated, depending on the host cell used.

The present studies were undertaken, therefore, to investigate the morphogenesis of the ribonucleoprotein of the Indiana strain of VSV in several human cell lines as well as BHK-21 cells. The results presented show that cytoplasmic inclusions consisting of filaments, identified as the ribonucleoprotein of VSV, can be produced depending on the host cell used for infection.

MATERIALS AND METHODS

Tissue culture. A BHK-21 line of Syrian hamster kidney cells was grown on monolayers in Blake bottles in a previously described medium (16), which consisted of a mixture of basal medium Eagle (BME, 2×) in Hanks balanced salt solution (HBSS), 10% fetal calf serum (FCS), and 10% tryptose phosphate broth.

Human amnion cells (AV_3) were purchased from Flow Laboratories, Inc., Rockville, Md, and human foreskin fibroblasts (HFS) were obtained through the courtesy of K. Paucker. Both lines were maintained as described for BHK-21 cells.

The RPMI-6410 (12) and SK-L1 (3) lymphoblastoid cell lines were grown and maintained as suspension cultures in medium RPMI 1640 supplemented with 10% fetal calf serum as previously described (23).

Virus. Plaque purified stocks of the Indiana strain of VSV were derived from infected BHK-21 cells. These preparations had titers ranging from 5×10^8 to 2×10^9 plaque-forming units (PFU)/ml.

Infection of cells with virus. Monolayers of cells (2×10^6) in 30-ml plastic tissue culture flasks were infected at a multiplicity of 10 in the medium described above. Virus was allowed to adsorb for 1 hr at 37 C, the monolayers were rinsed twice with HBSS, and fresh medium was added. The cultures were incubated at 37 C and harvested at given intervals.

For infection of lymphoblastoid cells, 10×10^6 cells were sedimented and resuspended in 1 ml of virus containing an input multiplicity of 10. After incuba-

tion, with intermittent shaking for 1 hr at 37 C, the cells were sedimented, washed twice with HBSS, resuspended in growth medium to a concentration of 10^6 cells per ml, and incubated at 37 C. Cultures were harvested 18 hr after infection.

Immunofluorescence assay. Monolayers of cells in 60-mm petri dishes, containing four cover slips (6 by 30 mm), were infected as described above. The cover slips were harvested at given intervals after infection. Preparation and staining of the lymphoblastoid cells, as well as of infected cover-slip cultures, have been described (9). All smears were stained with a fluorescein isothiocyanate-conjugated rabbit anti-VSV globulin.

Infectivity assay. Plastic petri dishes (60 mm) were seeded with BHK-21 cells in the above medium. They were incubated at 37 C in a 5% CO_2 atmosphere. Confluent monolayers were apparent after 24 hr. At this time, the medium was drained and the cells were inoculated with 0.2 ml of the various dilutions of virus. After an adsorption period of 1 hr at 37 C, the infected monolayers of cells were overlaid with 5 ml of medium supplemented with 1.2% Difco agar and neutral red at a final dilution of 1:40,000. The apparent plaques were enumerated 48 hr later, and titers were expressed as the number of plaque-forming units per milliliter.

Nucleoprotein extraction. A modified procedure similar to that described by Compans and Choppin (4) was used. Host cell ribonucleic acid (RNA) synthesis was inhibited by treating monolayers of BHK-21 cells with 1 μg of actinomycin D (Merck & Co., Inc, West Point, Pa.) per ml for 4 hr at 37 C (18). The monolayers were then rinsed and infected with VSV as described. After virus adsorption for 1 hr at 37 C, the cultures were refed with fresh medium containing uridine-5-^3H (Schwarz BioResearch, Orangeburg, N.Y.; specific activity, 20 Ci/mmole) at a concentration of 1 μCi/ml and incubated at 37 C. Sixteen hours after infection, the cells were harvested by scraping with a rubber policeman, pelleted by low-speed centrifugation, rinsed twice with phosphate buffered saline (7), resuspended in distilled water, and left at 4 C for 1 hr. The supernatant, after centrifugation at 900 $\times$ g for 20 min, was treated with deoxyribonuclease (20 μg/ml) for 30 min at room temperature, in the presence of Mg^{2+}, and then clarified by low-speed centrifugation. CsCl (2.0 g) was added to 4.5 ml of the resulting supernatant, and the solution was centrifuged at 140,000 $\times$ g for 24 hr in a Spinco SW 50 L rotor. Fractions were collected from the bottom in 0.17-ml amounts. The nucleoprotein-containing fractions were located by measuring radioactivity and optical density. For measuring radioactivity, 25-μliter samples were dispensed into vials containing Bray's solution (1) and counted in a Tri-Carb liquid scintillation spectrometer. Optical densities were determined in a DB spectrophotometer. Before examination in the electron microscope, fractions were dialyzed overnight at 4 C against 0.13 M NaCl, 0.05 M Tris (NT) buffer (pH 7.8).

Complement fixation. Complement fixation (CF) tests, were performed through the courtesy of S. Mazzur. Mouse ascites-fluids hyperimmune to VSV were kindly supplied by F. A. Murphy. The mouse hyperimmune fluids reacted both with coat and internal components of the virus but not with BHK-21 cell antigens. Titers were expressed as the reciprocal of the highest dilution of antigen showing complement-fixing activity, against 2 units of the hyperimmune fluids.

Electron microscopy. At the predetermined intervals, the medium was decanted from the cultures, the cells were washed with phosphate-buffered saline, and 1% phosphate-buffered osmic acid was added. After 5 min, cells were scraped into the fixative by means of a rubber policeman and were pelleted. The cell pellet was dehydrated in ethyl alcohol and embedded in epoxy resin. Thin sections were stained with lead citrate and uranyl acetate and examined in a Siemens Elmiskop at a magnification of $\times$10,500.

For examination by negative contrast, a drop of the dialyzed material was transferred to a carbon-coated Formvar grid by means of a platinum loop. A drop of phosphotungstic acid (pH 6.8) was added to this and the excess fluid removed by filter paper. The preparation was transferred into the electron microscope, while still moist, and viewed at a magnification of $\times$53,500.

RESULTS

Preliminary screening of cells. Four human cell lines, two monolayer, and two suspension cultures, as well as BHK-21 cells were infected with VSV at a multiplicity of 10. Table 1 summarizes the results obtained. Infectivity titrations, immunofluorescence, and thin-section electron microscopy were carried out 18 hr after infection. Although all cell lines tested produced viral antigens and infectious progeny, cytoplasmic inclusions were found only in SK-L1, RPMI-6410, and BHK-21 cells. Figure 1 is representative of the appearance of the inclusions 18 hr after infection with VSV. The major portion of the cytoplasm has been replaced by filamentous material. Normal cytoplasmic organelles were displaced and the filaments were found throughout the cytoplasm and in proximity to membranes from which virus could be seen budding.

Growth of VSV in BHK-21 and RPMI-6410

TABLE 1. *Screening of cells for inclusion formation 18 hr after injection with VSV*

Cell	Plaque-forming units/ml	Fluorescent cells	Inclusion formation
		%	
HFS	50.0×10^6	40	−
AV_3	30.0×10^6	70	−
SK-L1	5.0×10^6	40	+
RPMI-6410	8.5×10^6	70	+
BHK-21	$1{,}260.0 \times 10^6$	95	+

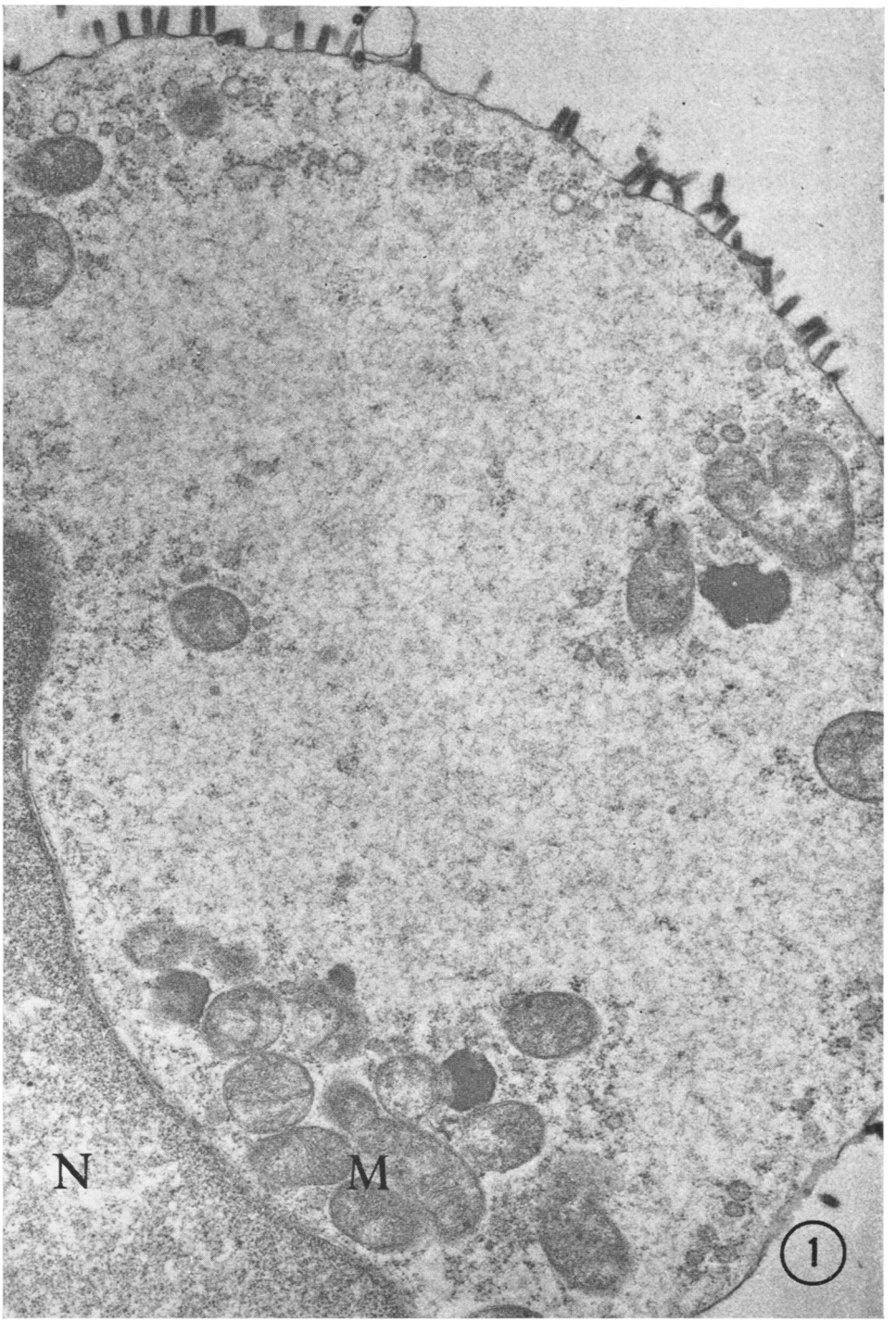

FIG. 1. *Representative cell (RPMI-6410) 18 hr after infection with VSV. The cytoplasmic matrix has been replaced by filamentous material. Virus particles can be seen budding on the plasmalemma. N = nucleus, M = mitochondrion.* × *21,000.*

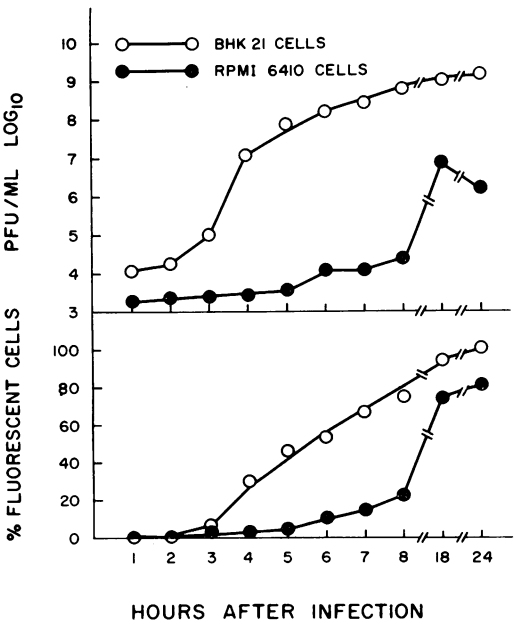

FIG. 2. *Development of infectious virus and virus-specific immunofluorescence in BHK-21 and RPMI-6410 cells infected with VSV.*

cells. A comparison of replication of VSV in one human cell line and in BHK-21 cells was investigated before studying the development of the inclusions. The viral replication was followed by infectivity titrations and immunofluorescence. The data presented in Fig. 2 show that in BHK-21 cells the first significant increase in virus infectivity and number of cells containing virus-specific immunofluorescence occurred between 3 to 4 hr after infection. Subsequently, a gradual increase in infectivity titer and number of fluorescent cells were observed, until maximum titers were reached 18 to 24 hr after infection. The replication of VSV RPMI-6410 cells was less efficient than in BHK-21 cells. Release of infectious progeny was slower and the amount of infectious virus produced was considerably less. Cells containing virus-specific immunofluorescence were not evident until 5 hr after infection, at which time only 4% of the cells were stained. The number of fluorescing cells and the production of infectious progeny did not increase significantly until 8 hr after infection. Maximum infectivity titers were reached at 18 hr. The greater permissiveness of the BHK-21 cells rendered them more suitable for the electron microscopic study. Subsequent studies on the development and nature of the inclusions were carried out therefore with BHK-21 cells.

Development of inclusions in BHK-21 cells. The morphological development of the cytoplasmic inclusions was studied in cell cultures harvested at hourly intervals from 3 to 8 hr after infection. The results paralleled those found using immunofluorescence (Fig. 2). In thin sections of cells 3 hr after infection, no inclusion formation nor virus reproduction were found. At 4 hr after infection, discrete foci of granular material (Fig. 3) could be seen in about 20 to 30% of the cells. The early inclusions appeared as areas of increased electron density readily distinguishable from the surrounding normal cytoplasm. At 5 to 6 hr after infection, a considerable number of cells contained these inclusions. Homogeneous masses composed of filamentous material could be found throughout the cytoplasm (Fig. 4); the inclusions were moderately electron dense, of varying size, and replaced the normal cytoplasmic constituents. Clusters of membrane-bound virus particles were found within or in close proximity to the inclusions. Virus particles also were seen budding from the surface membranes or into cytoplasmic vacuoles with filaments of the inclusions in close proximity (Fig. 5). A suggested relationship of the filamentous strands to the budding virus particles can be seen in Fig. 6. From 6 to 8 hr after infection, the morphological changes were enhanced and characterized by the formation in the cytoplasm of large areas of these filamentous masses which replaced normal cytoplasmic constituents, similar to that seen at 18 hr after infection (Fig. 1). The inclusions were not limited by membranes.

Neutralization of VSV with rabbit anti-VSV serum, before infection of cells, prevented formation of inclusions and production of infectious virus, as tested 8 and 18 hr after infection.

Isolation and identification of inclusion material. To relate the structures observed on thin sections of infected cells to the ribonucleoprotein of VSV, the material was extracted from the cells and subjected to various procedures for identification.

BHK-21 cells treated with 1 μg of actinomycin D per ml, infected with VSV, and labeled with ^{3}H-uridine were treated as previously described. After equilibrium centrifugation of the extracted material in CsCl for 24 hr, fractions were collected, and absorbancy and total counts were determined. The fraction containing the coincident peak of absorbency at 260 nm and radioactivity was dialyzed overnight at 4 C against NT buffer. Examination of this fraction by negative-contrast staining revealed the presence of single-stranded filaments. These filaments were further purified by recentrifugation to equilibrium in CsCl. Fractions were collected, the optical density at 260 nm, total radioactive counts, CF activity, and the density are shown in Fig. 7. The peak of absorbency (fraction 11) coincided with

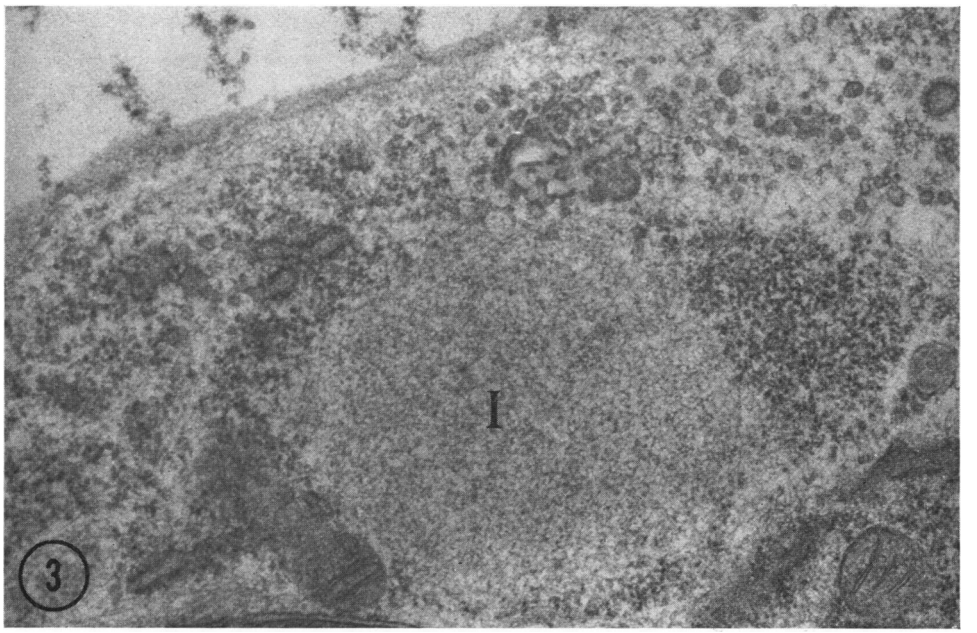

FIG. 3. *Inclusions (I) in BHK cells 4 hr after infection with VSV. × 30,500.*

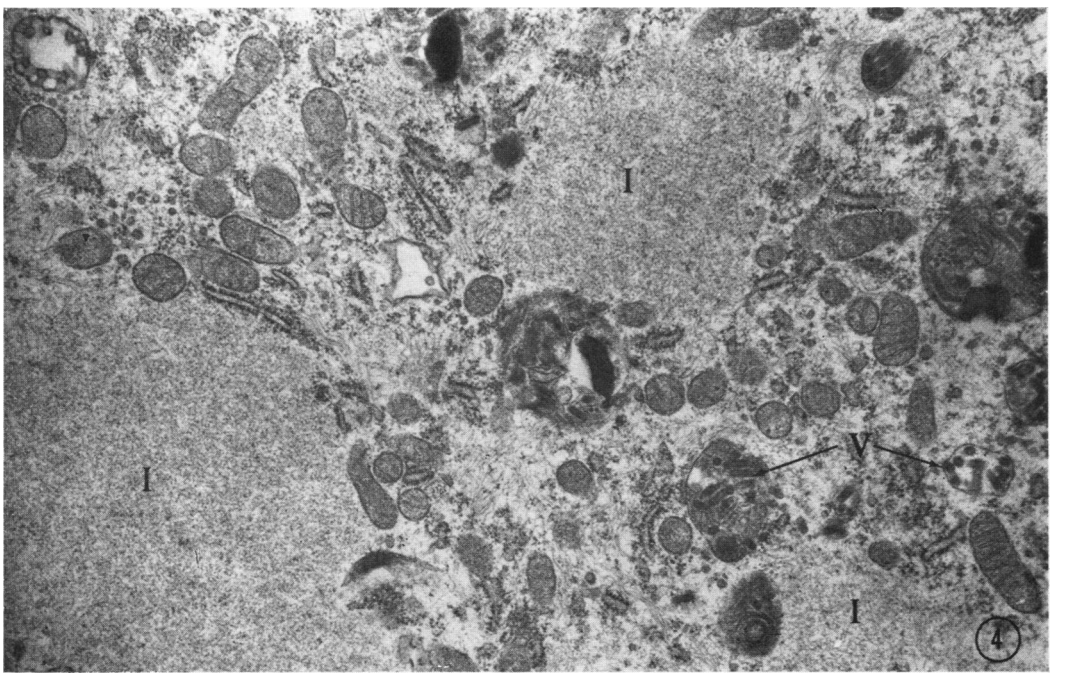

FIG. 4. *Appearance of inclusions (I) in the cytoplasm of BHK-21 cells 5 to 6 hr after infection. Filaments can be seen in the homogeneous masses and virus particles (V) bound by membranes are within or in close proximity to the inclusions. × 30,500.*

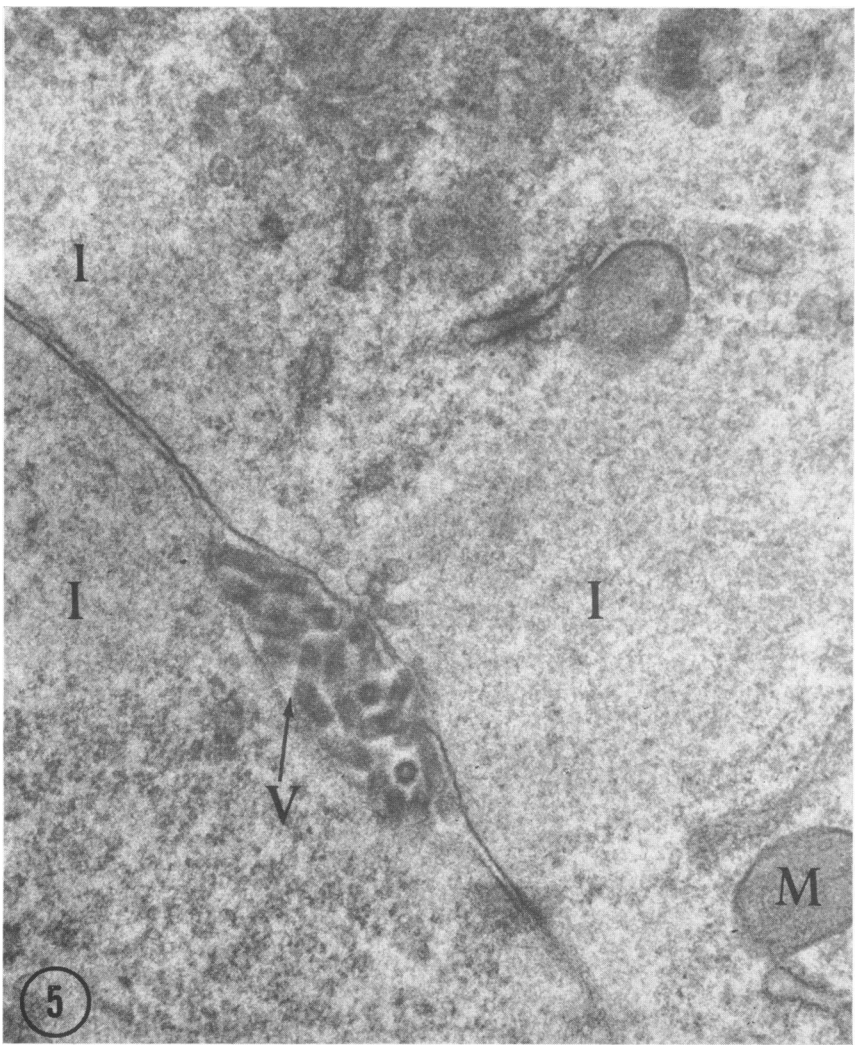

FIG. 5. *Filaments of the inclusions (I) underlying the cell membranes of BHK-21 cells next to virus particles (V).* × *52,500.*

that of the radioactivity incorporated into the filamentous component. A small contribution to absorbency and radioactivity was also seen in fractions 10 and 12, respectively. The buoyant density of the isolated strands (fraction 11) was 1.32 g/cm^3, as determined in repeated experiments. The virus-specific nature of the isolated strands was demonstrated by complement fixation by using specific anti-VSV mouse ascites fluids. The peak CF activity of 256 units/1.0 ml (fraction 11) coincided with the peak of absorbency and radioactivity. Fractions 10 and 12 each displayed 16 units of CF activity, whereas all other fractions were negative.

Examination of fractions 10, 11, and 12 by negative-contrast staining revealed the presence of single-stranded filaments. The strands isolated in fraction 11 are illustrated in Fig. 8A. Whether examined after the first or second banding in CsCl, they were always found as single strands. These were either loosely coiled or completely unwound and occasionally looped back on themselves. In none of the preparations examined were tightly coiled helices found. Occasionally, single stretched strands could be found that had an undulating appearance (Fig. 8B), the width of which varied from 2.5 to 8.5 nm, depending on the angle of viewing. Size variations were probably due to the geometry of the subunits which may be either rectangular or elliptical.

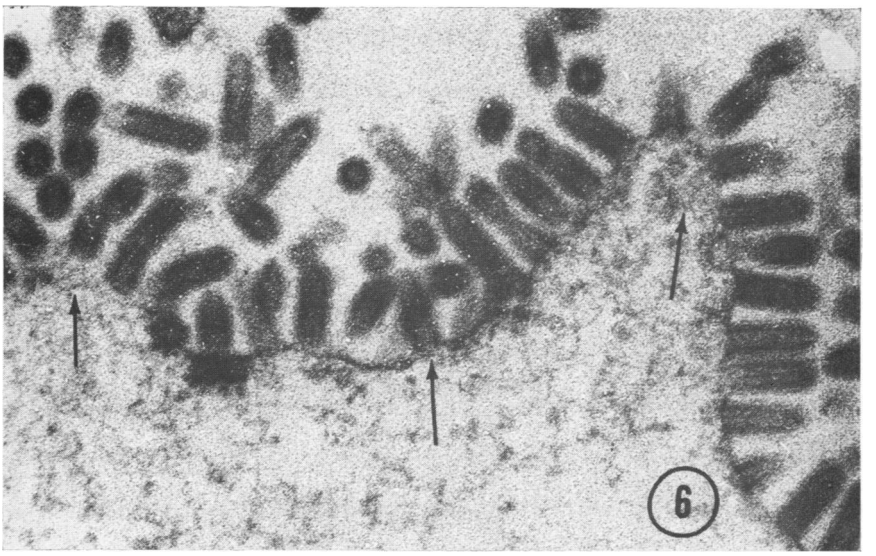

FIG. 6. *Filaments (arrows) in proximity to virus particles budding from the plasmalemma of a BHK-21 cell.* × *73,500.*

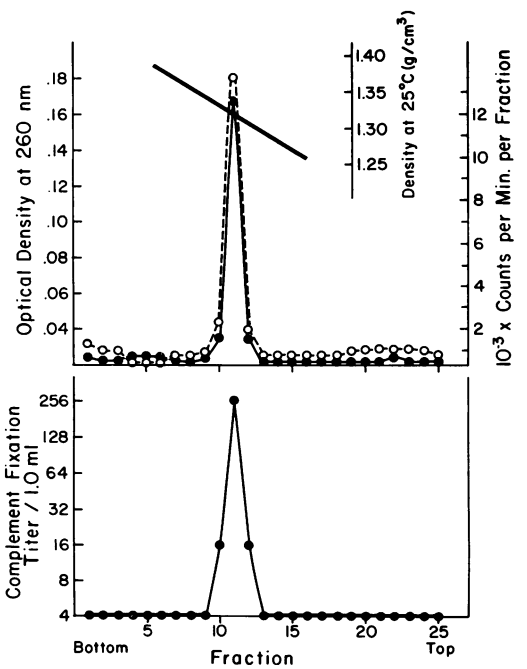

FIG. 7. *Equilibrium centrifugation in CsCl of nucleoprotein isolated from VSV-infected BHK-21 cells. Fractions were collected, the density (solid line), and total counts (●) are shown in the upper panel, as well as the optical densities at 260 nm (○) which were read after dilution of the fractions with 0.4 ml of NT buffer. The CF activity (●) of the fractions is presented in the lower panel.*

The ultraviolet-adsorption spectrum of the filamentous strands is shown in Fig. 9. The profile represented is indicative of the nucleoprotein nature of the material.

DISCUSSION

Wagner et al. (22) recently reported that the core protein (N) of VSV was synthesized in the cytoplasm of L cells in large intracellular pools. This N protein subsequently aggregated (presumably with progeny RNA) to form a sedimentable nucleocapsid. These aggregates were found in the cells from 2 hr after infection onward. The studies presented here demonstrate morphologically that cytoplasmic inclusions, consisting of filaments of viral ribonucleoprotein, were found in VSV-infected cells. The appearance of the inclusions was closely related to the development of virus-specific antigen as demonstrated by immunofluorescence. The filaments isolated from the inclusions contained ribonucleic acid and protein, demonstrated serological VSV-related activity, and had similar physical properties as the strands isolated from purified virions (15, 19, 21), i.e., a buoyant density of 1.32 g/cm³ and the appearance of undulating single strands which varied in width from 2.5 to 8.5 nm.

The nucleoprotein of VSV appeared to be much less structured than that of the tightly coiled helices of SV5 nucleocapsids isolated from infected cells (4). However, it was morphologically similar to rabies virus nucleocapsids (20). Simpson and Hauser (19) and Nakai and Howatson (15) have shown that as the nucleoprotein component of VSV was released from the virion the helix unwound to form an undulatory strand. The results suggested that the bonds which link the

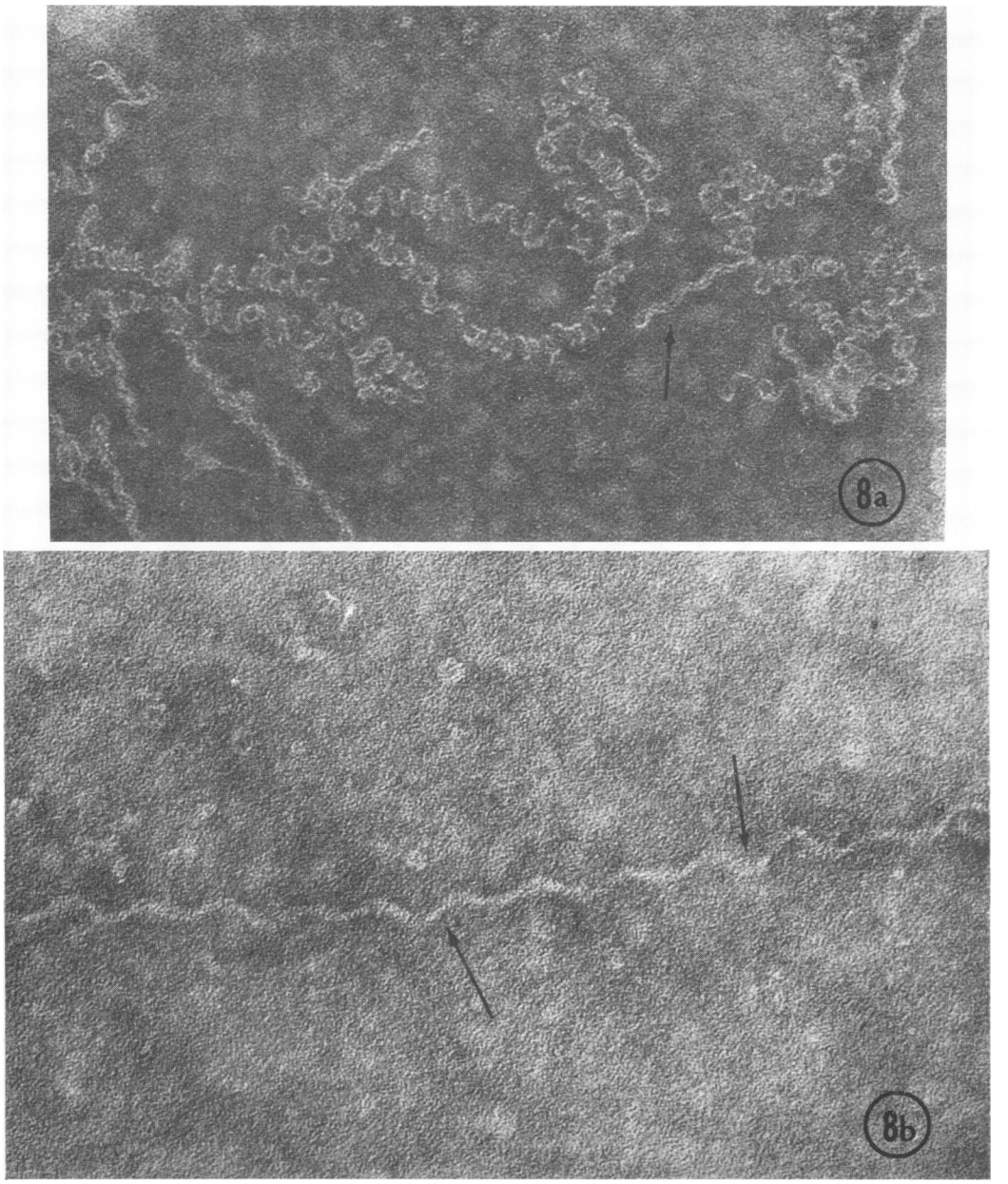

FIG. 8. *Nucleoprotein component isolated from VSV infected BHK cells after CsCl density gradient centrifugation. (a) Nucleoprotein showing different degrees of uncoiling. Part of a strand has looped back on itself (arrow). × 160,500. (b) Completely uncoiled nucleoprotein component. Arrows point out the difference observed in the width of the strand due to the angle of viewing. × 267,500.*

successive helical turns are more labile than the bonds which stabilize paramyxovirus nucleocapsids. The finding of only unwound strands in our preparations, derived from cells, indicated that the nucleoprotein did not exist as helices in the cytoplasmic inclusions. This was emphasized by the fact that the diameter of the strands when measured in thin section was approximately 9 nm, whereas the in situ helical nucleocapsid of VSV has a diameter of approximately 50 nm. These

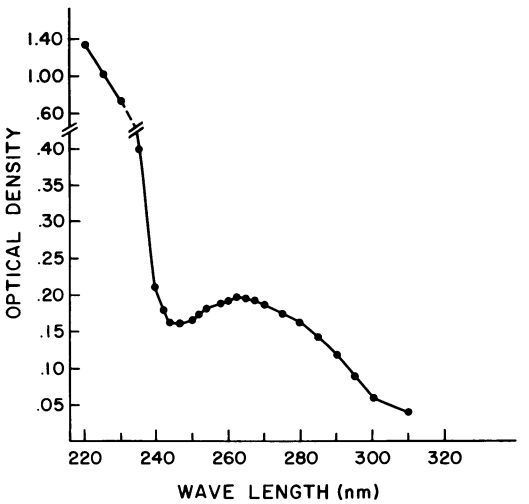

FIG. 9. *Ultraviolet absorption spectrum of purified VSV-nucleoprotein. Solvent: NT buffer; light path: 1 cm; protein content: 40 μg/ml.*

data suggest that the highly organized helical nature of the ribonucleoprotein component of the VS virion is acquired as the nucleocapsid is fed into the budding virion and does not exist as such a helical structure in the cytoplasm of infected cells.

The formation of the nucleoprotein inclusions was influenced by the host cell used. The reasons for the lack of inclusion formation in two of the cell lines and the mechanisms leading to the accumulation of the material in the other cell lines remain unclear. It has been shown with parainfluenza virus SV5 (5) that the accumulation of viral ribonucleoprotein was dependent on the host cell. When morphogenesis of the virus was an efficient process, the synthesis of nucleoprotein occurred at a rate equivalent to its incorporation into virions, and no accumulation occurred; however, minimal morphological differentiation of virus particles on the cell membranes resulted in nucleoprotein accumulation. This latter condition seems to be a reasonable explanation in the case of the lymphoblastoid RPMI-6410 cell. For this cell, production of infectious virus was delayed and less virus was produced per fluorescent cells as compared to BHK-21 cells. The development of infectious progeny in BHK-21 cells, however, did not differ in the time and amount produced as compared to permissive cells of other origins in which no accumulation of nucleoprotein had been observed (8). Virus particle differentiation, furthermore, did occur on all available cell membranes. Thus, the accumulation of large amounts of the nucleoprotein in the cytoplasm of BHK-21 cells did not seem to be a cell membrane-mediated phenomenon. The excess production of nucleoprotein in the fully permissive hamster cells may be caused rather by some alteration of the mechanism(s) responsible for the synthesis of this viral component.

ACKNOWLEDGMENTS

This investigation was supported by Public Health Service research grant AI-04911 and training grant AI-00104 from the National Institute of Allergy and Infectious Diseases.

The competent technical assistance of M. Cassel and N. Petruzzi is gratefully acknowledged.

LITERATURE CITED

1. Bray, G. A. 1960. A simple, efficient liquid scintillator for counting aqueous solution in a liquid scintillation counter. Anal. Biochem. 1:279–285.
2. Cartwright, B., C. J. Smale, and F. Brown. 1970. Dissection of vesicular stomatitis virus into infective ribonucleoprotein and immunizing components. J. Gen. Virol. 7:19–32.
3. Clarkson, B. D., A. Strife, and E. de Harven. 1967. Continuous culture of seven new cell lines (SK-L1 to 7) from patients with acute leukemia. Cancer 20:926–947.
4. Compans, R. W., and P. W. Choppin. 1967. Isolation and properties of the helical nucleocapsid of the parainfluenza virus SV_5. Proc. Nat. Acad. Sci. U.S.A. 57:949–956.
5. Compans, R. W., K. V. Holmes, S. Dales, and P. W. Choppin. 1966. An electron microscopic study of moderate and virulent virus-cell interactions of the parainfluenza virus SV_5. Virology 30:411–426.
6. David-West, T. S., and N. A. Labzoffsky. 1968. Electron microscopic studies on the development of vesicular stomatitis virus. Arch. Gesamte Virusforsch. 23:105–125.
7. Dulbecco, R., and M. Vogt. 1954. Plaque formation and isolation of pure lines with poliomyelitis virus. J. Exp. Med. 99:167–182.
8. Hackett, A. M., Y. C. Zee, F. L. Schaffer, and L. Talens. 1968. Electron microscopic study of the morphogenesis of vesicular stomatitis virus. J. Virol. 2:1154–1162.
9. Henle, G., and W. Henle. 1966. Immunofluorescence in cells derived from Burkitt's lymphoma. J. Bacteriol. 91:1248–1256.
10. Howatson, A. F., and G. F. Whitmore. 1962. The development and structure of vesicular stomatitis virus. Virology 16:466–478.
11. Hummeler, K., and H. Koprowski. 1969. Investigating the rabies virus. Nature 221:418–421.
12. Iwakata, S., and J. T. Grace, Jr. 1964. Cultivation *in vitro* of myeloblasts from human leukemia. N.Y. State J. Med. 64:2279–2282.
13. McCombs, R. M., M. Benyesh-Melnick, and J. P. Brunschwig. 1966. Biophysical studies of vesicular stomatitis virus. J. Bacteriol. 91:803–812.
14. Mussgay, M., and J. Weibel. 1963. Electron microscopic studies on the development of vesicular stomatitis virus in K.B. cells. J. Cell Biol. 16:119–129.
15. Nakai, T., and A. F. Howatson. 1968. The fine structure of vesicular stomatitis virus. Virology 35:268–281.
16. Russell, W. C. 1962. A sensitive and precise plaque assay for herpes virus. Nature 195:1028–1029.
17. Schulze, P., and H. Liebermann. 1966. Elektronenmikroskopische Untersuchungen zur Morphologie and Entwicklung des Virus der Stomatitis Vesicularis in Kalber-

nierenzellkulturen. Arch. Exp. Veterinaermed. 20:713–729.
18. Sedwick, W. D., and F. Sokol. 1970. Nucleic acid of rubella virus and its replication in hamster kidney cells. J. Virol. 5:478–489.
19. Simpson, R. W. and R. E. Hauser. 1966. Structural components of vesicular stomatitis virus. Virology 29:654–667.
20. Sokol, F., H. D. Schlumberger, T. J. Wiktor, H. Koprowski, and K. Hummeler. 1969. Biochemical and biophysical studies on the nucleocapsid and on the RNA of rabies virus. Virology 38:651–655.
21. Wagner, R. R., T. C. Schnaitman, R. M. Snyder, and C. A. Schnaitman. 1969. Protein composition of the structural components of vesicular stomatitis virus. J. Virol. 3:611–618.
22. Wagner, R. R., R. M. Snyder, and S. Yamazaki. 1970. Proteins of vesicular stomatitis virus: kinetics and cellular sites of synthesis. J. Virol. 5:548–558.